Springer Proceedings in Earth and Environmental Sciences

Tatiana B. Yanovskaya · Andrei Kosterov · Nikita Yu. Bobrov · Andrey V. Divin · Alexander K. Saraev · Nadezhda V. Zolotova *Editors*

Problems of Geocosmos—2018

Proceedings of the XII International Conference and School

Springer

Springer Proceedings in Earth and Environmental Sciences

Series Editor

Natalia S. Bezaeva, The Moscow Area, Russia

The series Springer Proceedings in Earth and Environmental Sciences publishes proceedings from scholarly meetings and workshops on all topics related to Environmental and Earth Sciences and related sciences. This series constitutes a comprehensive up-to-date source of reference on a field or subfield of relevance in Earth and Environmental Sciences. In addition to an overall evaluation of the interest, scientific quality, and timeliness of each proposal at the hands of the publisher, individual contributions are all refereed to the high quality standards of leading journals in the field. Thus, this series provides the research community with well-edited, authoritative reports on developments in the most exciting areas of environmental sciences, earth sciences and related fields.

More information about this series at http://www.springer.com/series/16067

Tatiana B. Yanovskaya · Andrei Kosterov ·
Nikita Yu. Bobrov · Andrey V. Divin ·
Alexander K. Saraev · Nadezhda V. Zolotova
Editors

Problems of Geocosmos—2018

Proceedings of the XII International Conference and School

Springer

Editors
Tatiana B. Yanovskaya
Saint Petersburg State University
St. Petersburg, Russia

Andrei Kosterov
Saint Petersburg State University
St. Petersburg, Russia

Nikita Yu. Bobrov
Saint Petersburg State University
St. Petersburg, Russia

Andrey V. Divin
Saint Petersburg State University
St. Petersburg, Russia

Alexander K. Saraev
Saint Petersburg State University
St. Petersburg, Russia

Nadezhda V. Zolotova
Saint Petersburg State University
St. Petersburg, Russia

ISSN 2524-342X ISSN 2524-3438 (electronic)
Springer Proceedings in Earth and Environmental Sciences
ISBN 978-3-030-21787-7 ISBN 978-3-030-21788-4 (eBook)
https://doi.org/10.1007/978-3-030-21788-4

This Springer imprint is published by the registered company Springer Nature Switzerland AG
The registered company address is: Gewerbestrasse 11, 6330 Cham, Switzerland

Preface

This volume is a collection of papers presented at the 12th conference and school "Problems of Geocosmos" held on October 8–12, 2018, at Peterhoff Campus, St. Petersburg State University. Organized primarily by faculty of the Department of the Earth Physics, this conference is one of the few in Russia to cover a broad range of geophysical research. In 2018, 140 scientists from Russia and abroad attended, including about 45 young scientists, graduate and undergraduate students.

The conference was organized into four parts: Exploration Geophysics (EG), Paleomagnetism, Rock Magnetism and Geomagnetism (P), Seismology (S), and Solar-Terrestrial Physics (STP).

Part EG has covered two broad areas of environmental and engineering geophysics: near-surface research and deep geoelectric studies. Five papers by EG part attendees are presented in this volume. Vorobev et al. discuss the problem of geomagnetically induced currents (GIC) and their influence on stable operation of electric power networks. The treatment is based on a statistical relationship between GIC and variations of the geomagnetic field. Ermolin and Ingerov introduce new methodological approaches to processing audio-magnetotelluric (AMT) and magnetovariational (MVP) data in a heterogeneous environment. Ermolin et al. consider possibilities for improving AMT data quality in the so-called dead band when measuring the AMT field at high latitudes. New theoretical developments in the field of magnetotelluric (MT) measurements and interpretation of MT data are presented in two papers by Plotkin and Mogilatov and Plotkin et al. The first paper considers a possibility to measure the vertical electrical component of electromagnetic field with the help of the circular electric dipole (CED). In the second paper, the possible influence of the Hall effect in MT sounding is discussed.

Part P provided a forum to discuss problems of paleomagnetism, rock magnetism, and geomagnetism. Nine papers in this volume cover the whole range of these topics. Grishchenko et al. and Guzhikov et al. discuss magnetostratigraphy of Valanginian parts in Crimea and Maastrichtian in the Lower Volga area, respectively. New paleomagnetic data are presented for the Lower Carboniferous of the South Urals (Golovanova et al.) and the Lower Cretaceous of the Amur terrane at the junction zone between Sikhote-Alin and Mongol-Okhotsk orogenic belts (Peskov et al.).

Kosterov et al. analyze magnetic hysteresis loops measured in strong, up to 7 Tesla, magnetic field on high-coercivity rock samples. Study of magnetic properties of fallow soils in Tatarstan is presented by Fattakhova et al. Two papers by Merkuriev et al. discuss applying marine magnetic anomaly data to geochronological and geo-historical analysis and to studies of non-dipole component of the Earth's magnetic field, respectively. Finally, Starchenko presents a method to obtain a simple estimate of the relationship between planetary convection and magnetism using scaling laws.

Presentations in Part S covered a wide range of problems, from global seismicity and new earthquake precursors to study of peculiarities of the Earth structure by seismic methods at different scales. Results of the development of new measuring devices were also presented. The papers in this volume reflect all the above-mentioned lines of investigation. Characteristics of the spatial–temporal distribution of the aftershocks are presented by Guglielmi et al. and Zotov et al.; distribution of seismicity in the Crimea is described by Gobarenko and Yegorova. A relationship between the ionospheric anomalies and strong earthquakes is studied by Korsunova et al. Three papers (Gobarenko et al., Yanovskaya et al., Krasnoshchekov and Ovtchinnikov) discuss new studies of the Earth structure covering, respectively, the Earth's crust, upper mantle, and core. New seismic instruments having an advantage of higher precision compared to the existing ones are described by Kislov and Gravirov, and Gravirov et al. The paper by Sharov presents a comprehensive overview of the results of superdeep drilling in Fennoscandia.

Part on Solar-Terrestrial Physics is traditional for "Problems of Geocosmos" conferences and is attended by participants from leading Russian research institutes and universities, and foreign research centers. Topics covered at STP Part include a wide range of magnetospheric, ionospheric, climatic, and solar studies. This volume contains contributions dealing with temporal relations in characteristics of the lower atmosphere and solar activity at the multi-decadal time (Veretenenko and Ogurtsov); pitch-angle diffusion coefficient of energetic protons on the basis of data of the THEMIS spacecraft (Popova et al.); temporal and spatial variability of geomagnetic and telluric electric fields in the Eastern Fennoscandia (Kozyreva et al.); the effect of auroral particle precipitation and polar cap patches on scintillations of the GPS signals in the polar ionosphere (Belakhovsky et al.). Based on the aa (and/or ap) indices, Sokolov et al. presented an improved catalogue of magnetic disturbances including storms with aa >30. Kopytenko et al. discussed possible origins of the displacement of the position of the auroral oval by more than 1500 km over the past 50 years. Remenets et al. reported results of the terrestrial electromagnetic sounding of the lowest part of ionosphere during the natural disturbances.

St. Petersburg, Russia
March 2019

Tatiana B. Yanovskaya
Andrei Kosterov
Nikita Yu. Bobrov
Andrey V. Divin
Alexander K. Saraev
Nadezhda V. Zolotova

Contents

Part I
Exploration Geophysics

Distortion of Local Magnetovariational Anomalies by Effect of Regional Structures

E. Ermolin and O. Ingerov

Abstract In this paper the authors consider the influence of the host medium on the morphology of the magnetovariational (MVP) anomaly from a local object with a relative conductivity of the section 10,000 Sm·m and 500 m depth. Conclusions are based on mathematical modeling. The results have shown that the covered rocks are the main cause of a local anomaly distortion. Resistivity changing of bottom layers have a weak effect on local anomaly disturbing. The anomaly of a local object can be isolated as a result of subtracting a regional component from the Wiese matrix of the original field. The express interpretation of MVP data and inversion codes can be applied for the described anomaly.

Keywords Magnetovariational method (MVP) · Induction vector · Tipper

1 Introduction

Two groups of methods are based on measuring the natural alternating electromagnetic (EM) field of the Earth: magnetotelluric (MT) [1] and magnetovariational (MVP) [2]. In the MT sounding method 4 horizontal components (Ex, Ey, Hx, Hy) are measured. In the MVP method 3 orthogonal magnetic components (Hx, Hy, Hz) are studied. Both methods can be operated independently, but it is more expedient to use them together. This 5-component EM method is an effective tool for solving a wide range of geological exploration tasks.

The response functions in the MVP method are the induction vector and the tipper [2]. Earlier it was shown that by means of using the singular points on the pseudo-sections of the tipper, it is possible to quickly estimate the parameters of 2D and 3D anomalous objects of a simple geometric shape [3, 4]. The algorithms

E. Ermolin (✉)
GM Service, Saint-Petersburg, Russia
e-mail: e.ermolin.gms@gmail.com

O. Ingerov
Phoenix-Geophysics, Toronto, Canada
e-mail: olexandr_ingerov@yahoo.ca

T. B. Yanovskaya et al. (eds.), *Problems of Geocosmos—2018*, Springer Proceedings in Earth and Environmental Sciences, https://doi.org/10.1007/978-3-030-21788-4_1

developed by the authors can be called "the method of express-interpretation of magnetovariational data". This technique has been developed for a homogeneous half-space. But in real conditions we deal with a complex environment and the responses of various geological objects are superimposed on each other. Large lateral inhomogeneities of the Earth's crust and the upper mantle create anomalies. The MVP method can find these anomalies at a distance of up to several hundred kilometers. As a result, the response from the local searched object is considerably distorted, and it becomes impossible to apply the express interpretation methods. At the same time, it is interesting to separate the local component from the regional influence. The current state of this problem is described by Berdichevsky and Dmitriev [1]. On the qualitative level, for the first time the division of the regional and local components of the real part of the induction vector was performed in the work [5]. The quantitative interpretation of the separated local component is an unresolved issue nowadays. The purpose of this work is to estimate the influence of different variants of the horizontally layered host medium and regional 2D conductors on the parameters of the anomaly created by a local body of a simple geometric shape. The most important goal is the answer to the question: is it possible to use the separated local part for further quantitative interpretation?

2 Methods and Modeling Results

We have performed mathematical modeling by means of the WinGLink software [6]. 2D anomalous body of a regular geometric shape is taken as a basic geoelectrical model. Within the framework of this paper the parameters of the anomalous local object have not been changed (the cross section of the body (200 × 200 m), the resistivity (4 Ω·m), the depth to the upper edge (500 m). The object was placed in a horizontally layered medium, shown in Fig. 1. The model consists of several key elements: a sedimentary cover with the thickness of 200 m and the resistivity of 20 Ω·m (total longitudinal conductivity of 10 Sm), a conductive layer of 1 km thickness (resistivity 20 Ω·m and 500 m depth to the upper edge), the boundary of the Earth's crust (M) and the boundary of the lithosphere sole (L).

The studies were divided into 3 stages. At the first stage, the response from the model presented in Fig. 1 was analyzed. At the second stage the influence of the host medium on the local anomaly was estimated. At the third stage, the influence of a 2D regional conductor located at a distance from 40 to 0.4 km from a local object was estimated. As a regional conductor, the suture zone model is taken. Similar objects are often found in the Earth's crust [7].

At the first stage the most significant pseudo-sections of the MT and MVP responses, calculated from the basic model (Fig. 1a) were analyzed. The object clearly appears in the MT and MVP response in spite of the presence of an overlapping cover. In the impedance phase of the TE-mode, the object is displayed on 2 period ranges (Fig. 1c). The first range is around 0.02 s (the amplitude of the anomaly is 6°). The second range is around 2 s (the amplitude of the anomaly is 3°). On the

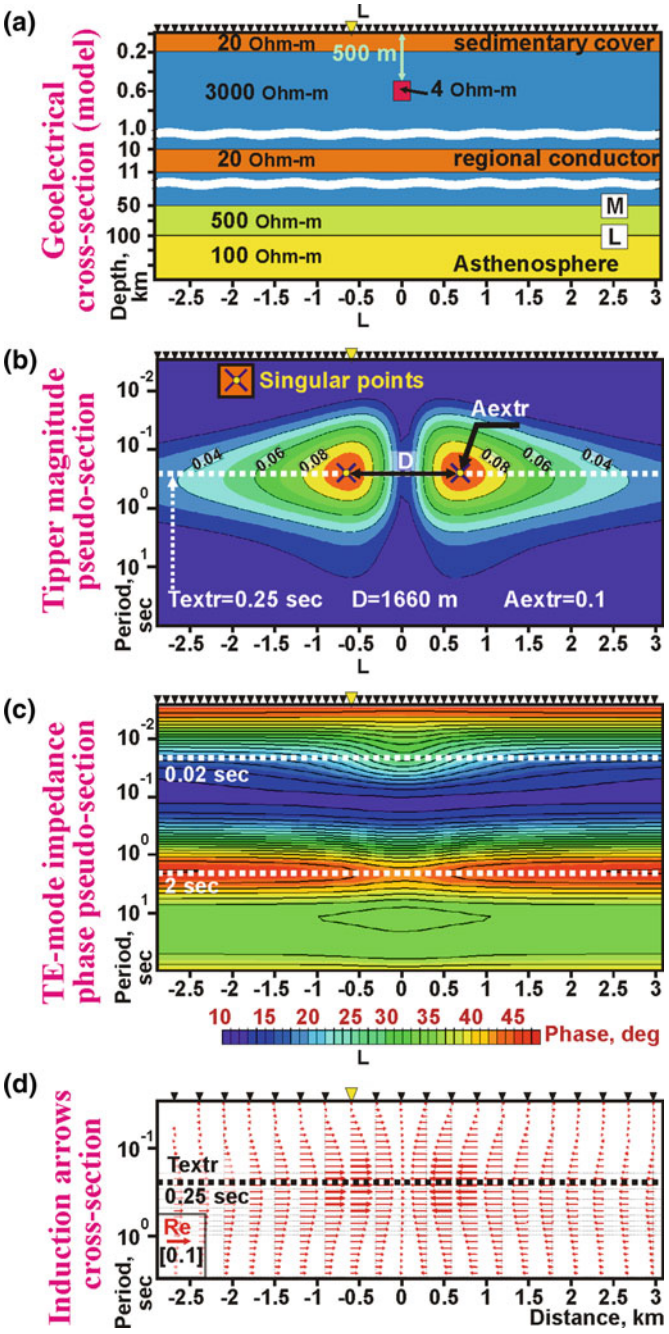

Fig. 1 Geoelectrical basic model (**a**), Pseudo-sections of the response functions (**b–d**)

section of induction vectors (Fig. 1d), the anomalous body appears at a period of 0.25 s. In case of using both MT and MVP methods, the object appears over a wide range of periods (3 decades). In practice, you can use the range where the data quality is better. It should be noted that using the data of induction vectors (pointing to the conductor), the presence of an anomalous body and the direction to it can be detected at a distance of 2 km (Fig. 1d). The TE-mode anomaly attenuates at a distance of 0.7 km.

On the tipper pseudo-section (Fig. 1b), the object appears as a paired anomaly having 2 maxima (2 singular points) with the amplitude of 0.1 at the period Textr = 0.25 s. The distance between two singular points (D) is 1660 m. In previous work [3] the authors gave formulas for an operative estimation of the anomalous conductivity of the cross section (G) and the depth of the geometrical center of the anomaly body (H):

$$G = \gamma \cdot T, \tag{1}$$

$$H = \alpha \cdot D + c, \tag{2}$$

where γ is a coefficient in Sm·m/s; α is a non-dimensional coefficient; c is a coefficient in m. G is the parameter of the anomaly 2D body, which is determined as the multiplication of the cross sectional area of the 2D anomaly body and the anomalous electrical conductivity of the 2D anomaly body [3]. It is measured in Sm·m.

The anomaly object presented in the previous work [3] was placed in homogeneous half-space with 3000 Ω·m resistivity. The cross section of the anomaly body was 200 × 200 m, the resistivity was 4 Ω·m. The G of that object was equal to 10,000 Sm·m. The thin layer (thickness 25 m) at the top of the model with resistivity 100 Ω·m has been added (total longitudinal conductivity of 0.25 Sm). In previous work authors proved linear dependencies (1) and (2). The coefficients γ, α and c were determined. The coefficient γ is equal to 2×10^5 Sm·m/s. The coefficient α is equal to 0.46. The coefficient c is equal to 154 m.

As the result of using Formula (1) the G of the anomaly object is equal to 50,000 Sm·m. Using this formula, the G value of the object presented in Fig. 1a increased five times relatively to real G (10,000 Sm·m). Obviously, the difference is caused by the difference in the host medium. In the second stage of the investigation the influences of the several types of host-medium have been studied.

At the second stage of the study, the thickness and resistivity of the covered rocks and the resistivity of the asthenosphere were changed in the model from Fig. 1a. In addition, the influence of a regional conductor located at a distance of 40 km was estimated. The model of the suture zone [7] was taken as a regional conductor. We compared the parameters of singular points (period—Textr, maxima amplitude—Aextr and the distance between the maxima—D) on the tipper cross-sections calculated from different geoelectrical models. The results of the comparison are shown in Table 1. It can be seen that if total conductivity of overlapping rocks changes, the parameters of the singular points (Textr, D, Aextr) on the tipper cross-section alter

Table 1 Changes of the singular points parameters under the influence of varying the model shown in Fig. 1a

a Difference in singular points for models with 0.25 Sm and 10 Sm

Period (**Textr**)	Distance (**D**)	Amplitude (**Aextr**)
66.94 %	358 m	0.287

b

		Local body	Local body, asthenosphere resistivity 1 Ohm-m	Local body and suture zone
25 m cover, 100 Ohm-m (0.25 Sm)	**Textr** (change)	0.248 s	0.250 s (0.81%)	0.249 s (0.20 %)
	D (change)	1276 m	1283 m (7 m)	1280 m (4 m)
	Aextr (change)	0.098	0.098 (0)	0.096 (0.002)
200 m cover, 20Ohm-m (10 Sm)	**Textr** (change)	0.082 s	0.082 s (0.37%)	0.081 s (0.91%)
	D (change)	1665 m	1656 m (9 m)	1634 m (31 m)
	Aextr (change)	0.385	0.385 (0)	0.393 (0.008)

considerably (Table 1a). There are no fundamental changes of singular points parameters in the case the asthenosphere resistivity changes. It is more important that there is no change in the case of adding the suture zone, situated 40 km away from the local object, in the cross-section (Table 1b).

At the third stage the suture zone was located at a different distances from the local anomaly. The influence of the regional conductor on the local anomaly was analyzed more detailed. The geoelectrical models for the distances of 40, 7.5 and 0.4 km are shown in Fig. 2a. The tipper magnitude pseudo-sections calculated from the models are shown in Fig. 2b. The parts of the tipper magnitude pseudo-sections where the local anomaly appears are shown in Fig. 2d. The white isolines illustrate the response of the local anomalous body without the suture zone presence. The results of the calculation in case of the local body absence are shown in Fig. 2c. If the regional structure is located at a distance of 40 km from the local anomalous object (Fig. 2a-1), the anomaly morphology from the local object is practically not distorted. This can be seen from a detailed examination of the pseudo-section of the tipper (Fig. 2d-1). White isolines reflect the shape of the anomaly. Therefore, we can use express-interpretation methods.

When an anomalous object is located at a distance of 7.5 km from the suture zone (Fig. 2a-2), the low-period part of the anomaly of the local object is distorted (Fig. 2d-2). We can not determine the parameters of singular points, but the presence of a local object can be assessed at a qualitative level by the presence of a less distorted high-frequency part of the anomaly. Figure 2 in section e-2 shows the projections of

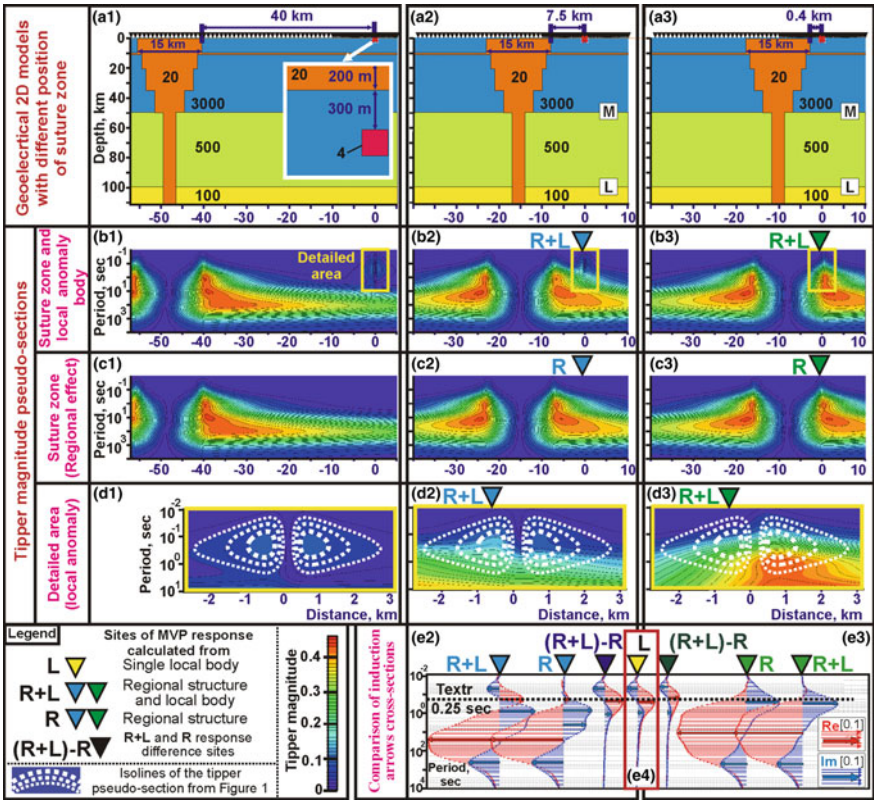

Fig. 2 2D geoelectrical models (**a**); pseudo-sections calculated from models containing: a local body and a regional structure (**b**, **d**), only a regional structure (**c**); projections of real (red vectors) and imaginary (blue vectors) parts of induction vectors in the Parkinson convention (pointed to conductor) (**e**)

the real and imaginary parts of induction vectors calculated for the model shown in Fig. 2a-2. Curves R + L correspond to the models where both a regional conductor and a local object present. The R curves are calculated only for the regional conductor (there is no local object). The curve L (Fig. 2e-4) is calculated only for a local object (there is no regional structure). It can be seen that the local object on the R + L curve is clearly visible at the period of 0.25 s. Moreover, the value of the maximum period and the amplitude of the vectors coincide with the curve L. We performed a subtraction of the values of the components of the matrix R from the components of the Wiese matrix R + L for all frequency range. The final curve is presented in the same section in Fig. 2e. This is the curve of the vectors (R + L) − R. If the curves of the induction vectors (R + L) − R and L have to be compared, it is difficult to visually distinguish them. Consequently, after dividing the regional and

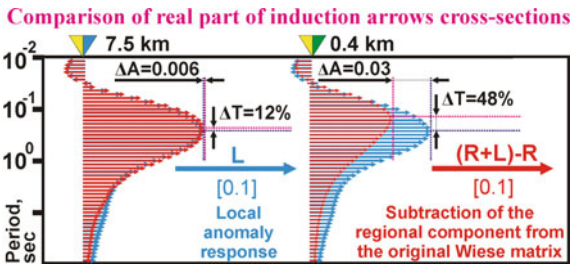

Fig. 3 Comparison of induction arrows

local parts by subtracting the components of the Wiese matrix, we can apply the express-interpretation or inversion technique to the magnetovariational data.

If the regional object is located at a distance from a local object less than its depth (Fig. 2a-3), it is practically impossible to determine the presence of a local object even at a qualitative level. Nevertheless, with the formal subtraction (R + L) − R, we obtain a curve of the vectors that does not in principle differ from the vectors of the local object (L). A more detailed comparison of the real part of induction arrows between L and (R + L) − R curve for 7.5 and 0.4 km separation of the local body and the suture zone is shown in Fig. 3.

If the distance between the regional structure and the local object is less than the depth to the upper edge, the difference of (R + L) and L curve of induction arrows is greater than the field measurement error.

3 Conclusions

The modeling results have shown that for the local anomalous object with a relative conductivity of the cross section of 10^4 Sm·m and a depth to the upper edge of 500 m, the following conclusions are valid:

1. The host medium affects the morphology of the magnetovariational anomaly. The morphology of the anomaly is primarily related to the parameters of the sedimentary cover.
2. If the local and regional anomaly can be visually separated, the presence of large remote regional conductors in the studied area has a very weak effect on the shape of the anomaly from the local 2D object.
3. The local magnetovariational anomaly, distorted by regional anomalies, can be highlighted by simple subtracting the regional constituent of the components of the Wiese matrix from the original field.

The possibility to separate local and regional parts of anomalous signal in magnetovariational method was demonstrated for synthetic data, calculated from current geoelectrical model. Application this approach for real field data is the target of future investigations.

References

1. Berdichevsky, M.N., Dmitriev, V.I.: Models and methods of magnetotellurics, 564 p. Springer, Berlin, Heidelberg (2008)
2. Rokityansky, I.I.: Geoelectromagnetic Investigation of the Earth's Crust and Mantle, 381 p. Springer, Berlin, Heidelberg (1982)
3. Ingerov, O., Ermolin, E.: The parameters estimation of 2D conductive isometrical bodies by singular points at the tipper frequency characteristic. In: IAGA WG 1.2 on Electromagnetic Induction in the Earth 20th Workshop Abstract, Giza, Egypt (2010)
4. Ermolin, E., Ingerov, O., Fox, L.: MTS and MVP data integration to estimate the 2D anomaly bodies parameters situated away from measuring profile. In: 22-th EM Induction Workshop Weimar, Germany (2014)
5. Lozovoy, A.L., Mendry, Y.V., Ingerov, I.: Localization of the position of conducting anomalous objects with the help of local and regional real induction vectors. In: 14th EAGE Conference & Exhibition, Almaty, Kazakhstan (2018)
6. WinGLink Homepage. https://www.slb.com/services/seismic/seismic-reservoir-characterization/electromagnetics/emsoftware/winglink.aspx. Accessed 2019/02/13
7. Feldman, I., Erinchek, Yu., Egorov, A.: Scientific and methodological problems of the geological interpretation of a digital database of materials of deep electrical exploration in the territory of the European part of Russia. Zapiski Gornogo Instituta **176**, 154–158 (2008). (in Russian with English abstract)

The Features of Dead Band AMT Signal in Chukotka Region

E. Ermolin, O. Ingerov, A. A. Yankilevich, N. N. Pokrovskaya, T. V. Davytkina and V. Melnikov

Abstract In this paper we analyze the amplitude spectra of the audiomagnetotelluric (AMT) natural-source signal. Special attention is given to the signal in the frequency range from 1 to 5 kHz known as "dead band". We study the measurements of the base sites that were used during summer fieldwork in 2013, 2014 and 2017 in Chukotka Region (Russian Far East). The area is located above the Arctic Circle. As it has been described by previous researchers, the stable signal in the dead band can be acquired only at nighttime. We would like to point out that in the daytime the local maximum at 2.4 kHz frequency is observed within the dead band in Chukotka. The 2.2 and 2.6 kHz frequencies can be reconstructed by using more than 3 h of daytime data acquisition. These frequencies can be used as the ranging marks. These ranging marks sometimes allow reconstructing the AMT curve by using the relationship between the amplitude and phase. We present a proposal for improving data quality in the dead band during the daytime.

Keywords Magnetotellurics · Magnetovariational profiling · EM monitoring · Amplitude spectra · Dead band

1 Introduction

Magnetotelluric sounding (MT) and magnetovariational profiling (MVP) methods [1] are based on measuring five components of the natural alternating electromagnetic field of the Earth. This technique is a reliable instrument for solving a large number

E. Ermolin (✉) · V. Melnikov
GM Service, Saint-Petersburg, Russia
e-mail: e.ermolin.gms@gmail.com

O. Ingerov
Independent Expert, Toronto, Canada
e-mail: olexandr_ingerov@yahoo.ca

A. A. Yankilevich · N. N. Pokrovskaya · T. V. Davytkina
Saint-Petersburg Mining University, Saint-Petersburg, Russia
e-mail: yankilevich@mail.ru

T. B. Yanovskaya et al. (eds.), *Problems of Geocosmos—2018*, Springer Proceedings in Earth and Environmental Sciences, https://doi.org/10.1007/978-3-030-21788-4_2

of exploration tasks. For investigation at small depths (less than 2 km), the high-frequency modification of magnetotelluric method—AMT (audiomagnetotellurics) is applied. In the AMT modification, the frequency range from 10 kHz to 1 Hz is used depending on the modification of magnetic sensors. It is considered that the source of the field in AMT is thunderstorms in equatorial regions. The peculiarity of this source is that the minimum of the signal amplitude is presented in the frequency range from 1 to 5 kHz. The specified range is called "dead band". An extensive study of this problem is found in Xavier Garcia and Alan G. Jones article [2]. For enhancing data quality in the dead band they propose the following: 1. Perform a sounding at night; 2. Increase the sensitivity of magnetic sensors; 3. Use more than one reference point for processing. At present, a new approach has appeared: using dispersion relationship in the magnetotelluric tensor in the first stage of data processing [3]. Unfortunately, it is hardly ever feasible to apply all the given recommendations. However, the information about the curve in dead band is very important for many exploration tasks.

We performed AMT survey for gold exploration in Chukotka [4]. The geological task demanded obtaining AMT data of a very high quality, because the search objects (gold-bearing quartz veins) are small (thickness from 1 to 5 m). The veins are covered with a layered volcanic rock cover with a thickness of 80–300 m.

The investigated area is located above the Arctic Circle where the signal in the dead band is much weaker. All regular measurements were done by using remote reference station technique [5]. Despite this, we could not get good quality AMT data in the dead band during the daytime. Nighttime measurements were the only way to acquire adequate data in the high-frequency band. That decreased the productivity of the fieldwork significantly. Nevertheless, some measurements were carried out in the daytime in the hope of obtaining AMT curves of an adequate quality. In July and August, it can be done with a 50–70% chance and in October with a 10% chance.

The purpose of this investigation was to search for the features of the amplitude spectra of 5 field components (Ex, Ey, Hx, Hy, Hz). Some features will probably help to find new ways of enhancing the AMT and MVP data quality in the dead band.

2 Methods

We used the records of the remote reference sites in the periods of fieldwork in Chukotka: August–October 2013; June–September 2014; July–August 2017. The natural field was registered daily for 15 h from 12:00 to 8:00 local time. The averaged coordinates of the area are: Longitude: 170° E, Latitude: 70° N. MTU-5A receivers, AMTC-30 magnetic coils and the non-polarized lead electrode by "Phoenix-Geophysics Ltd" were used. The magnetic sensors were installed on the tripods manufactured by "AGCOS Inc". All the cables and tripods were buried in the base site. At the 24 kHz sampling frequency, 4 records in each of 10 s timeslot were used. The results of data acquisition (time series) were divided into 30-min intervals. SSMT2000 software was used for data processing. Estimates of impedance

(apparent resistivity, magnetic or electric field spectra) with auto electric reference (local E) [5] were used. In this article we consider only the year 2017 data, because the main conclusions of three seasons data analysis have not got principle differences.

3 The Data Analysis and Results

We visualized the results of data processing. The analysis has been done for: I—amplitude spectra as the function of time; II—the curves of amplitude spectra (for a more detailed analysis); III—amplitude at the frequencies 3 and 1.5 kHz; IV—analysis of AMT apparent resistivity curves. All considered data refer to one site.

I. The amplitude spectra for 5 components as the function of time are shown in Fig. 1 (August, 2017). In the dead band, the clear periodicity of the signal amplitude is observed which is connected with a certain time of the day. This blue-purple band of the low level of all components in the frequency band from 6 to 0.9 kHz contracts and expands over time. It gets widest (the lowest amplitude) from 12:00 to 15:00 (in the daytime) and the most narrow (the maximum amplitude) from 00:00 to 03:00 (at night). The day of August, 11, stands out in the average regularity. On this day an abnormally large amplitude spectral value is observed throughout the day. The dead band is shown more detailed in Fig. 2 from 8 to 13 of August in the frequency range from 10 to 0.1 kHz.
   In Fig. 2 the general minimum of the amplitude spectra in the dead band is observed in the daytime. But at the same time, the local maximum is observed at frequency 2.4 kHz within the general minimum. This local maximum is more visible in the vertical magnetic component. Over here the two local minimums of the dead band are clearly visible: 3 and 1.5 kHz.
   We also visualized the amplitude of signal curves as a function of frequency to analyze the features of amplitude spectra in the daytime more detailed.

II. Frequency characteristics of a 4-h daytime record on August, 8 (from 12:30 to 16:30), and a short 30-min night record on August, 9 (from 02:00 to 02:30), are shown in Fig. 3. These are typical spectra in the field seasons of 2013, 2014 and 2017. In Fig. 3 it is clearly seen that the amplitude spectra at night is higher than those in the daytime. In Fig. 3 the local maximum is clearly observed on daytime spectra in the dead band at the frequencies 2.2 and 2.6 kHz. This local maximum is marked by a transparent blue square in Fig. 3. The table in Fig. 3 demonstrates that the amplitude spectra of the local maximum in the dead band are higher by 85% (relative to the values of two nearby local minimums). Thus, there is a strong possibility that the AMT curve can be rebuilt at the local maximum using the daytime record. The presence of the local maximum in the dead band can be an indicator of sufficient data quality in the daytime. Consequently, for daytime measurements it is essential to carry out an operative analysis of the

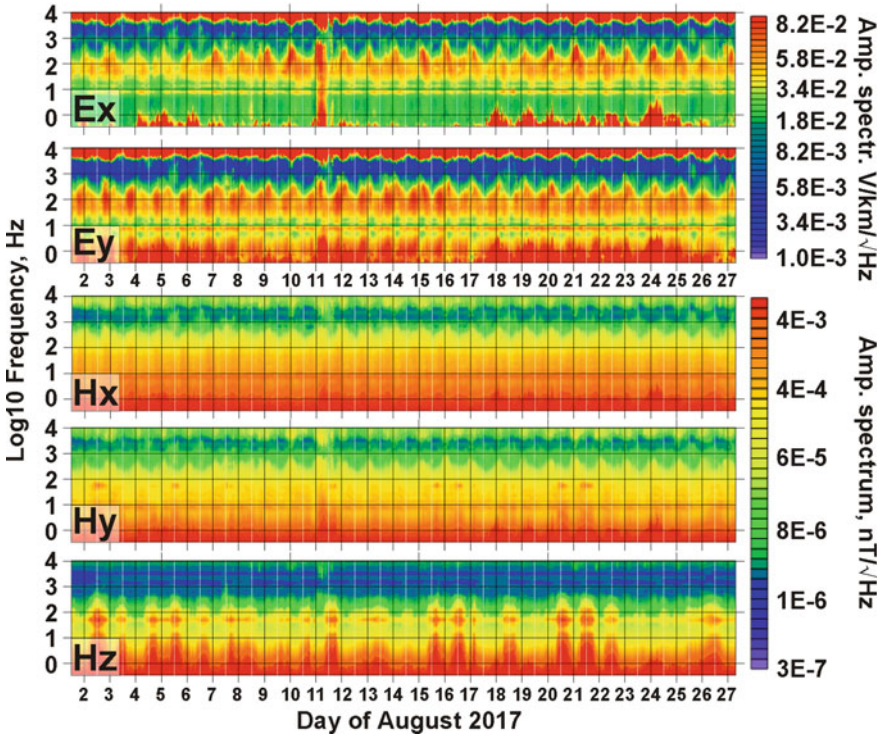

Fig. 1 AMT amplitude spectra in August, 2017

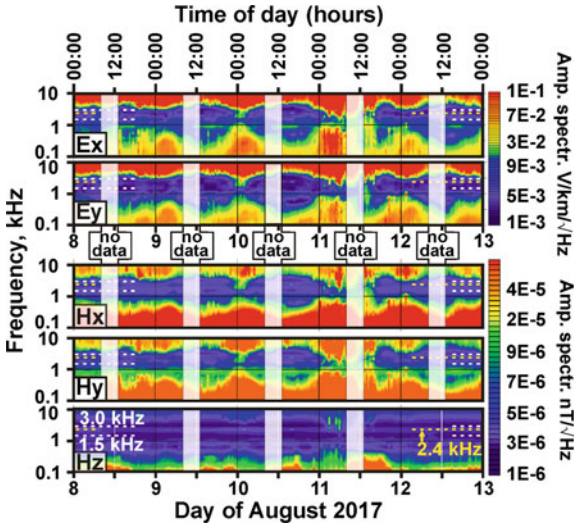

Fig. 2 Amplitude spectra from 8 to 13 of August

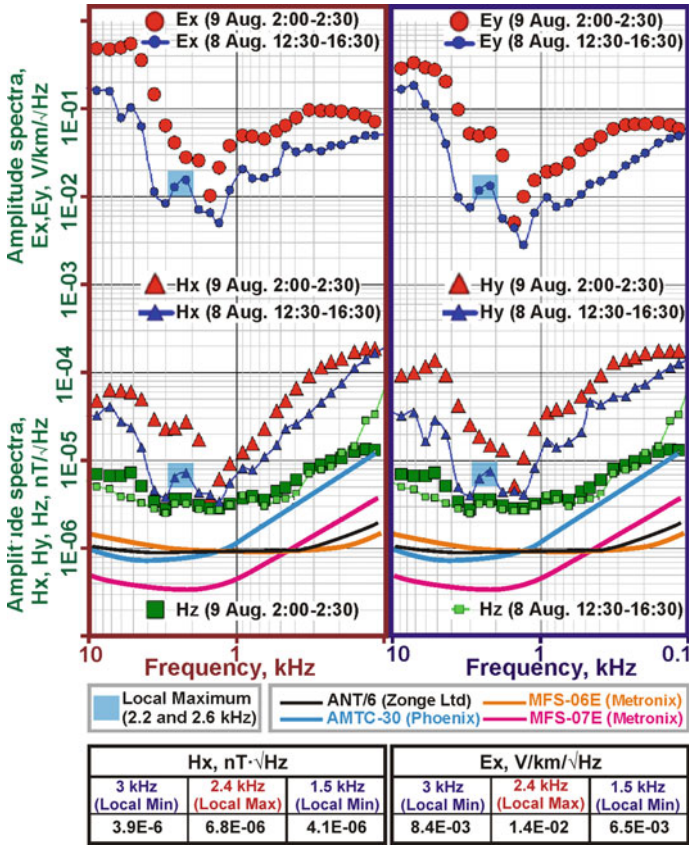

Hx, nT·√Hz			Ex, V/km/√Hz		
3 kHz (Local Min)	2.4 kHz (Local Max)	1.5 kHz (Local Min)	3 kHz (Local Min)	2.4 kHz (Local Max)	1.5 kHz (Local Min)
3.9E-6	6.8E-06	4.1E-06	8.4E-03	1.4E-02	6.5E-03

Fig. 3 The comparison of the amplitude spectra measured at night and in the daytime. Sensors noise characteristics are shown as color lines (the manufacturer's website official data). Hx and Ex local maximum and two local minimums amplitude values in the daytime are shown in the table

amplitude spectra and other impedance functions immediately after recording in field conditions.

It should be noted that in the dead band the amplitude of magnetic components is lower than that of electric components (relative to 100 Hz frequency). Therefore, the noise in magnetic channels is greater than noise in electric channels. For this reason, in the investigated area for the dead band we used the estimates of impedance with remote electric reference (Remote E) [5]. The comparison between the natural-signal amplitude levels and official characteristics of sensors noise of the commonly used sensors are shown in Fig. 3. This figure illustrates that the own noise of modern magnetic sensors is significantly lower than the natural-signal amplitude in the dead band. Consequently, the dead band problem is not connected with the sensor noise but in a greater degree with external noise. As a result, a crucial task is to improve the ways of sensor installation

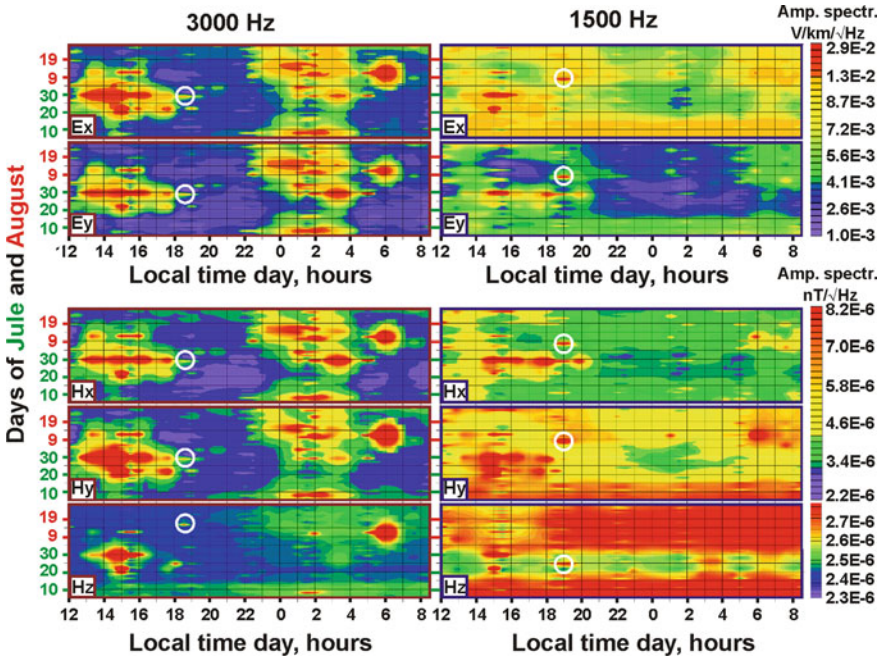

Fig. 4 Dependence of the signal amplitude in the local time of the days from July, 4, to August, 26, at frequencies 1.5 and 3 kHz. Local maximums are shown with white circles

to decrease external noises. Due to high noises in the magnetic channels, the values of apparent resistivity appear to be substantially smaller. This is what we observe in the dead band.

III. The signal amplitudes at 1.5 and 3 kHz have minimal values in the dead band. For this reason, we performed a detailed analysis of these frequencies specifically. The results are shown in Fig. 4. At 3 kHz frequency the signal is higher at night from 0:00 to 4:00 for all components. Also, from July, 15, to August, 15, the increased values are observed from 13:00 to 17:00 local time. At 1.5 kHz frequency the signal level is higher in the daytime. At night from 22:00 to 5:00 the values are low. That is why the frequency 1.5 kHz is the most challenging problem concerning the dead band.

Single local anomalies of the increased amplitude values deserve special attention (the white circles in Fig. 4). They chaotically appear throughout the day. We used the MTU-5A receivers, where at a sampling frequency of 24 kHz, in fact only 2–5% of the measurement time is recorded. The increasing of the sampling frequency and the recording of continuous time series will probably help to measure the rare "pulses" of the signal. It is likely that this technique will help to partially solve the problem with the data quality of AMT curves in the dead band.

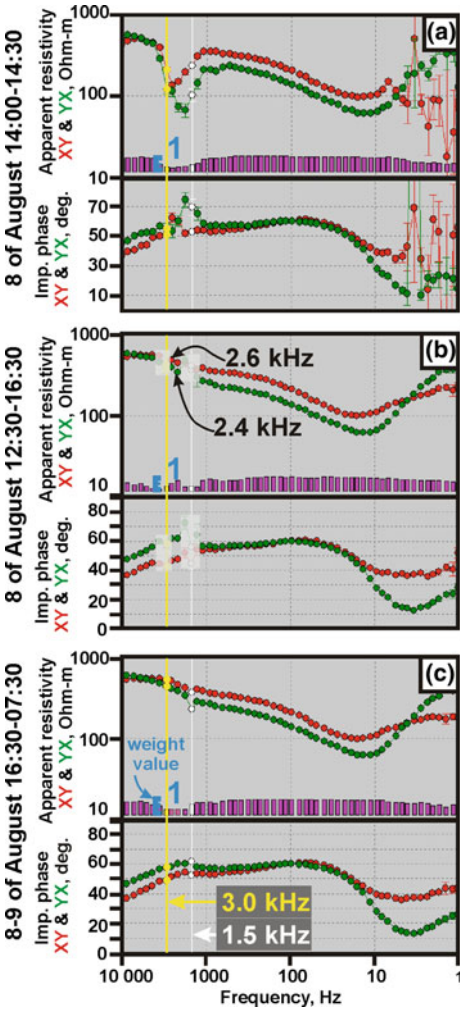

Fig. 5 Apparent resistivity curves and impedance phases for: a 30-min (**a**) and 4-h (**b**) daytime record on August, 8; 15-h night record on August, 8–9 (**c**). Chukotka region

IV. The apparent resistivity curves and impedance phase curves of AMT are shown in Fig. 5 for a short daytime record (5a), 4-h daytime record (5b), and 15-h record (5c). The remote-reference processing was applied.

The curve in Fig. 5a is a rejected take because the amplitude and phase values at 11 consecutive frequencies in the dead band deviate significantly from the real curve.

The curve in Fig. 5b is of much better quality. Its main feature is that the amplitude and phase values at frequencies of the local maximums (2.2 and 2.6 kHz) can be restored as a result of the interactive rejection of solutions with a low weight. Due to the presence of these benchmarks, we can restore the apparent resistivity curve in the dead band. As a rule, the values that significantly deviate

from the general level of the curve (1–2 frequencies above and 2–3 frequencies below) are removed in practice. After that, the dispersion relationship between the amplitude and the magnetotelluric impedance phase are used. This procedure is called "amplitude-phase correction" [6]. Some authors implement this procedure at the stage of primary data processing [3]. The basic idea is that the amplitude and the phase in the same frequency range carry information about different depths (the phase is responsible for the deeper part of the section). It should be noted that this procedure is correct only for the areas where there are no obvious violations of the dispersion relations in the impedance tensor. The curve in Fig. 5c is of adequate quality. We can use this curve for analysis and interpretation just after removing only the value at 1.5 kHz.

4 Conclusions

We have analyzed the AMT amplitude spectra in the dead band in Chukotka summer fieldwork. Local maximums within the dead band in the daytime (frequencies 2.2 and 2.6 kHz) have been described. The daytime records can be used only if the curve in the local maximums (2.2–2.6 kHz) can be reconstructed. As a rule, for "Phoenix-Geophysics ltd" MTU-5A equipment it is necessary to carry out measurements in the daytime for not less than 3 h. Also, no more than 2–3 frequencies on both sides of the local maximum should be defective.

It is possible that the continuous registration of time series at high frequencies and improving the ways of magnetic sensor installation will allow decreasing measurement length in the daytime and increasing data quality in the dead band. In the field works it is currently important to perform operative visualization of impedance parameters immediately after performing measurements on the site.

References

1. Berdichevsky, M.N., Dmitriev, V.I.: Models and methods of magnetotellurics, 564 p. Springer, Berlin, Heidelberg (2008)
2. Garcia, X., Jones, A.: Atmospheric sources for audio-magnetotelluric (AMT) sounding. Geophysics **67**, 448–458 (2002)
3. Jones, A.: Magnetotellurics: status quo and quo vadimus. DMEC Exploration 2017 Abstr 11, 139–158 (2017)
4. Ermolin, E., Ingerov, O., Savichev, A.: Gold exploration in Chukotka region by using audio-magnetotellurics. In: 22-nd EM Induction Workshop, Weimar, Germany Abstr (2014)
5. Gamble, T.D., Goubau, W.M., Clark, J.: Magnetotellurics with remote reference. Geophysics **44**, 53–68 (1979)
6. Feldman, I., Ermolin, E.: Amplitude-phase correction of magnetotelluric impedance curves. Zapiski Gornogo Instituta **194**, 200–210 (2011). (in Russian with English abstract)

Role of Hall Effect in Magnetotelluric Sounding

Valery V. Plotkin, Vladimir S. Mogilatov and Vladimir V. Potapov

Abstract Many minerals belong to the semiconductor class from the point of view of the mechanism of electrical conductivity. One of the experimental methods for determining the electrical conductivity of semiconductor minerals is based on the Hall effect. Due to the presence of the Earth's magnetic field it is possible to expect the manifestation of this effect in natural conditions during electromagnetic soundings. To detect manifestations of the Hall effect during magnetotelluric (MT) sounding, a polarization analysis method is proposed, based on a data processing algorithm that divides the time spectrum of the MT field into normal mode spectra with right and left circular polarization. Numerical estimates and results of a special field experiment are presented.

Keywords Magnetotelluric sounding · Hall effect · Normal modes · Right and left circular polarizations

1 Introduction

Host rocks overlaying oil and gas deposits penetrated by a stream of hydrocarbon fluids, represent a semiconductor medium in which manifestation of the Hall effect is possible [1]. Interest in this phenomenon arose from the results of electromagnetic soundings with controlled sources in hydrocarbon-rich areas [2]. Similar phenomena may be observed during electromagnetic soundings of porous geological media due to the effect of the Earth's magnetic field on currents in fluids. Here the role of viscosity is large, and viscosity coefficient can be determined from the experiment.

V. V. Plotkin (✉) · V. S. Mogilatov · V. V. Potapov
Institute of Petroleum Geology and Geophysics SB RAS, Koptug Ave. 3, Novosibirsk 630090, Russia
e-mail: PlotkinVV@ipgg.sbras.ru

T. B. Yanovskaya et al. (eds.), *Problems of Geocosmos—2018*, Springer Proceedings in Earth and Environmental Sciences, https://doi.org/10.1007/978-3-030-21788-4_3

2 The Polarization Analysis Method

So far, for geological media the characteristics of microprocesses are insufficiently known, therefore it is better to address an experiment. For its planning, it is possible to consider the influence of the Earth's magnetic field by introducing the Hall conductivity σ_H into the electrical conductivity tensor. In an anisotropic medium, the field splits into two components, called normal modes, which differ in attenuation coefficients and phase velocities. The difference between modes is connected with its polarization and direction of rotation of the field vector; in the first mode the field rotates clockwise, in the second counterclockwise. For physical reasons, it is clear that due to Hall effect the response of the medium may be different in the case of excitation of the medium by only one of the normal waves.

Analysis of MTS data shows that generally the direction of rotation of MT-field vectors (right or left polarization) is defined by characteristics of frequency spectrum. It is well known that polarization is generally elliptic, and at different frequencies, the direction of rotation of field vector is determined by the phase difference of spectral elements of horizontal components at different frequencies. So, if we assume the field time dependence in the form $e^{i\omega t}$ and introduce the designations $H_x(\omega) = A_x(\omega)e^{i\varphi_x}$ and $H_y(\omega) = A_y(\omega)e^{i\varphi_y}$, then the horizontal component of magnetic field vector rotates clockwise when $\sin(\varphi_y - \varphi_x) > 0$, and counterclockwise when $\sin(\varphi_y - \varphi_x) < 0$. This can be explained by the ratio of amplitudes of normal modes with circular polarization representing the MT-field.

The mode amplitudes can be determined using a polarization analysis of time spectrum of MT-field. For this purpose, it is necessary to know the polarization coefficients for a given mode. The calculations carried out in [3] for the horizontally layered medium with the parameters $\sigma_n, h_n, n = 1, \ldots, N, h_N \to \infty$ showed that in middle latitudes mode polarizations coefficients in all layers are close to $\pm i$ when $\sigma_H \ll \sigma_n$. It means that under these conditions modes with right or left circular polarization are normal. Then, for any elliptic polarization, the decomposition of MT-field into modes with right and left circular polarizations can be performed using the following representation for the real part of horizontal components:

$$Re\{H_x(\omega)e^{i\omega t}\} = Re\{A_x(\omega)e^{i(\varphi_x+\omega t)}\} = A_1\cos(\varphi_1+\omega t) + A_2\cos(\varphi_2+\omega t),$$

$$Re\{H_y(\omega)e^{i\omega t}\} = Re\left\{A_y(\omega)e^{i(\varphi_y+\omega t)}\right\} = A_1\sin(\varphi_1+\omega t) - A_2\sin(\varphi_2+\omega t),$$

where the mode with index 1 is characterized by the counterclockwise rotation of magnetic field horizontal components, and the mode with index 2 by the clockwise rotation. Amplitudes and phases of modes are then calculated using the polarization analysis formulas:

$$H_{1,2}(\omega) = A_{1,2}e^{\varphi_{1,2}},$$